BIFURCATION AND STABILITY ANALYSIS OF BISTABLE NEUROMODULES

Stephen Lynch* and Jon Borresen
School of Computing, Mathematics and Digital Technology
Manchester Metropolitan University,
Manchester, M1 5GD, UK
Email: s.lynch@mmu.ac.uk

arXiv:1606.07307v2 [math.DS] 19 Sep 2016

Abstract

This paper presents a stability analysis of simple neuromodules displaying fold bifurcations (leading to hysteresis), flip bifurcations (period doubling and undoubling to and from chaos) and Neimark-Sacker bifurcations (quasiperiodic and periodic bifurcations). For the first time, bifurcation diagrams are plotted using a feedback mechanism. It is shown that the stability curves and bifurcation diagrams must be dealt with simultaneously in order to fully understand the dynamics of the systems involved. Synaptic weights, biases and gradients of transfer functions are varied and the system is shown to be history dependent. The work can be applied to artificial neural networks and developing brains and gives a very important generalization of previous work in this field.

Keywords: Artificial Neural Network; Bifurcation; Neuron

* Corresponding author.

E-mail: s.lynch@mmu.ac.uk

1. Introduction

In recent times, the disciplines of neural networks and dynamical systems have increasingly coalesced and a new branch of science called neurodynamics is emerging. This paper is primarily concerned with a simple nonlinear two-neuron module displaying bistable behaviour, but other nonlinear phenomena have to be discussed in order to fully understand the dynamics involved. The paper deals with discrete models, but the dynamics of continuous and stochastic models are important and will now be briefly discussed.

The basic model of a cell membrane is that of a resistor and capacitor in parallel. The differential equations used to model the membrane are a variation of the van der Pol equations and represent a simple continuous system. The famous Fitzhugh-Nagumo oscillator [1, 2], used to model the action potential of a neuron, is a two-variable simplification of the Hodgkin-Huxley equations [3]. The integrate and fire neuron modelling the slow collection and fast release of voltage is a biologically inspired model of a neuron and matches the qualitative behaviour very well. The authors are currently investigating new computer architectures using such coupled oscillator dynamics [4]–[7]. This recent work on coupled Hodgkin-Huxley equations with time delayed synaptic coupling, demonstrates controlled switching between synchronized cluster states, leading to reliable logic based programming derived from a biological model. This work should have significant implications for understanding neural encoding with applications in novel computation. In 1982, Hopfield [8] showed how an analog electrical circuit could behave as a small

network of neurons with graded response. He derived a suitable Lyapunov function for the network to check for stability, and used it as a content-addressable memory.

More recently, the authors have had UK and international patents published on binary oscillator computing [9, 10]. Arithmetic logic and memory have been demonstarted using Fitzhugh-Nagumo threshold oscillators to perform binary logic [11]. They are currently seeking industrial partners to investigate possible technological implementations using Josephson junctions as the threshold oscillators.

It is well known that time continuous systems are often investigated in terms of their discrete time analogues. Using approximations and algorithms from numerical analysis, a discretized version of the differential equations used to model neuron dynamics can be computed [12]. One popular method for producing discretized versions of higher dimensional continuous systems involves constructing Poincaré maps, see [13]–[15], for example.

The mechanism of stochastic resonance was introduced in the early 1980's by Benzi et al. [16]. The nonlinear effect of stochastic resonance at first appears to be counterintuitive—a random noise can make a system sensitive to an otherwise undetectable signal. In practice, there is normally an intermediate noise level which makes the signal transmission optimal [17]. Under certain conditions, noise can improve signal transmission properties of neuronal systems [18]. In general, a two-state model is enough to exhibit the main features of stochastic resonance. Zaikin et al. [19] show that noise induces jumps between different steady states in a bistable system. Drover and Ermentrout [20] analyzed a nonlinearly coupled system of bistable differential equations and showed that there are jumps between critical points and limit cycles. Lynch and Christopher [21] have demonstrated multiple bistable loops for certain highly nonlinear differential equations used to model wing rock in modern aircraft and surge in jet engines. For these systems, there are jumps from limit cycles to limit cycles as certain parameters vary.

Chaotic and periodic behaviour has been observed in the human brain, see [22]–[24], for example. In terms of mathematical models, Pasemann and his research group have published a number of papers on simple neuromodules analysing their bistability, chaos, chaos control, synchronization, periodicity and quasiperiodicity, [25]–[29]. Yuan et al. [30], study the stability and bifurcation analysis of a discrete-time network for a single fixed point in terms of Neimark-Sacker bifurcations with special classes of transfer function. They list parameter values where the fixed point is stable and using the normal form method and the centre manifold theory for discrete systems developed by Kuznetzov [31], they give an algorithm for determining whether a bifurcation from the fixed point is subcritical or supercritical. In 2008, Guo et al. [32] extended this work and considered a simple discrete two-neuron network with three delays. They derive necessary and sufficient conditions for the asymptotic stability of a fixed point and investigate the existence of three types of bifurcation, namely, flip bifurcation, fold bifurcation and Neimark-Sacker bifurcation. Redmond et al. [33], consider a general class of first-order nonlinear delay-differential equations with reflectional symmetry and apply the theory to simple models from neural networks and atmospheric physics. Their analysis reveals a Hopf bifurcation curve terminating on a pitchfork bifurcation line at a codimension-two Takens–Bogdanov point in parameter space. X. Xu [34], investigates local and global Hopf bifurcation in a two-neuron module with two distinct delays. In all of the papers above, the analysis is restricted to a single fixed point.

It has long been known that simple neuronal models can display steady-state behaviour, periodic behaviour, quasiperiodic behaviour and chaos. One major factor that has been overlooked in studying simple neuromodules is feedback. The two essential ingredients for bistability, or hysteresis, are nonlinearity and feedback [9]–[13]. Both of these processes are inherently present in neuronal dynamics. Bistable behaviour often occurs in physical systems for only a narrow range of parameter values and hence can be difficult to observe. Mathematical analysis can be used to test for stability, and bistable and unstable regions can be plotted for a range of

parameter values. Bistable phenomena have been proven to exist in a wide range of physical forms. They are present in biological systems [35, 36], human brain dynamics [37], economics [38], mechanical systems [39], electric circuits [11], chemical kinetics [41], astrochemical cloud models [42], psychology [43, 44], neural networks [45] and nonlinear optics [46, 47], where optical bistability has potential applications in high speed all-optical signal processing and all-optical computing. Parameters such as weights, biases and gradients of transfer functions can be altered when an artificial neural network is learning. Biologically, these same variables obviously go through similar changes as the biological brain develops.

Section 2 is concerned with the mathematical model of a single neuron considered by Pasemann [26], and a simple two-neuron module is investigated in Section 3. The analysis can be seen to match very well with the numerical results displayed in bifurcation diagrams incorporating a feedback mechanism, however, there are exceptional cases which have not been discussed elsewhere. Conclusions and further work will be discussed in Section 4.

2. Stability analysis of a single neuron

The simple chaotic neuron investigated by Pasemann [26] is modelled using the discrete equation

$$x_{n+1} = b + \gamma x_n + w\sigma(x_n), \tag{1}$$

where x_n is the activation level at time n, b is a bias, w is a self-weight and, $0 < \gamma < 1$, is a decay rate depicting the dissipative property of a real neuron. The output is given by the unipolar transfer function, $\sigma(x) = 1/(1 + e^{-x})$. This system can display hysteresis and period-doubling bifurcations to and from chaos. This system cannot display quasiperiodic behaviour. Fixed points of period one satisfy the equation

$$x = \gamma x + b + w\sigma(x),$$

where x is the fixed point of period one. The stability edges for x occur when $|f'(x)| < 1$, $f(x) = b + \gamma x + w\sigma(x)$. Thus, the fixed point is stable as long as

$$|\gamma + w\sigma'(x)| < 1.$$

The parametric equations defining the stability boundaries are given by

$$B^{+1}: \quad b = (1-\gamma)x - \frac{1-\gamma}{1-\sigma(x)}, \quad w = \frac{1-\gamma}{\sigma'(x)},$$

$$B^{-1}: \quad b = (1-\gamma)x + \frac{1+\gamma}{1-\sigma(x)}, \quad w = -\frac{1+\gamma}{\sigma'(x)},$$

where B^{+1} defines the bistable boundary, where fixed points undergo fold bifurcations. The curve depicted by B^{-1} determines where the system goes unstable, and fixed points undergo flip bifurcations. The parametric curves are plotted in Figure 1 when $\gamma = 0.5$. In this case, the bistable region is isolated from instabilities.

Bistable behaviour for the single neuron is demonstrated in Figures 2(a) and 2(b). In Figure 2(a), the bias b is ramped up from $b = -5$ to $b = 5$, and then ramped down again. One parameter is varied and the solution to the previous iterate is used as the initial condition for the next iterate; in this way, a feedback mechanism is introduced. In this case, there is a history associated with the process and only one point is plotted for each value of the parameter. This method has been labelled as the second iterative method by Lynch [13]–[15]. The bistable region matches with the results of the linear stability analysis given in Figure 1. In Figure 2(b), a larger bistable region is produced as both parameters, b and w, are increased and then decreased simultaneously. It should be pointed out at this stage that in most physical situations many

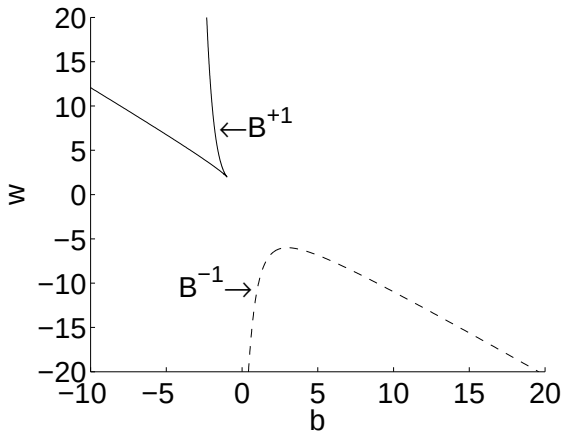

Figure 1: Stability diagram for the nonlinear neuron when $\gamma = 0.5$. The curve B^{+1} is the boundary for bistable operation and the curve B^{-1} is the border for period-doubling bifurcations.

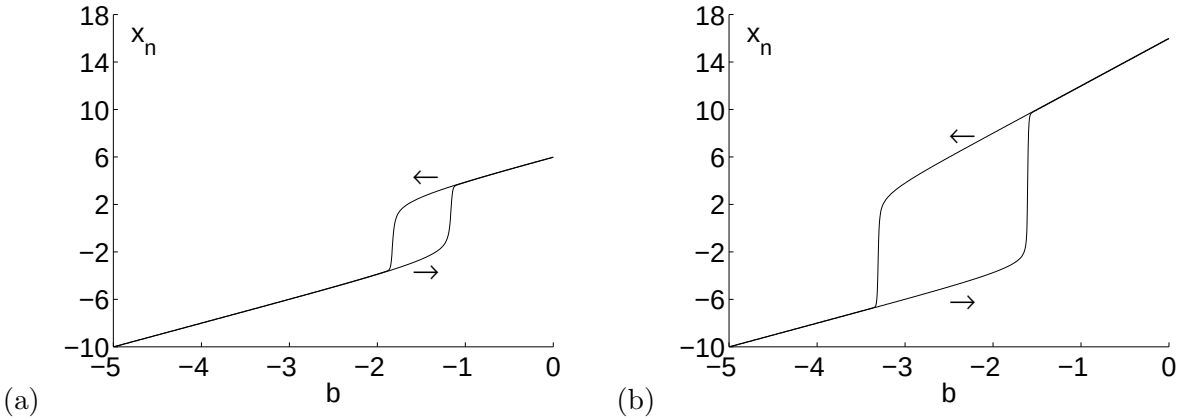

Figure 2: Bifurcation diagrams for system (1) when $\gamma = 0.5$ using a stepsize of 0.01. (a) The bias b is ramped up from -5 to 0 and then ramped down again, the parameter w is fixed at $w = 3$. (b) The bias b and weight w are ramped up and down simultaneously, $-5 \leq b \leq 0$ and $3 \leq w \leq 5$.

parameters would be varying simultaneously and it is only in rare cases that most parameters would be kept constant as one parameter is varied.

Figures 3(a) and 3(b) show bifurcation diagrams for system (1), when $\gamma = 0.5$ and the parameter b is ramped up and down, $(-5 \leq b \leq 5)$, and parameter w is simultaneously ramped down then up, $(-10 \leq w \leq 10)$. In Figure 3(a), the initial condition chosen at $\gamma = 0.5, b = -5, w = 10$ was $x(0) = -10$, however, in Figure 3(b) the initial condition chosen for the same set of parameter values was $x(0) = 10$. In Figure 3(a), there is a small bistable region for b close to -1, which shrinks as the step size used in the iterative scheme is decreased. For increasing values of the parameter b, the solution remains on the steady-state even though the fixed point becomes unstable at $b \approx 3$. As the parameter b is decreased, from $b = 5$, the solution becomes unstable (a stable period two orbit) and then returns to the steady-state at $b \approx 3$, once more, where it remains as b is ramped back down to $b = -5$ and w is ramped back up to $w = 10$. In Figure 3(b), there is a large bistable region for $-5 < b < -1$, approximately. For increasing values of the parameter b, the solution again remains on the steady-state on the upper branch of the hysteresis cycle. As the parameter b is decreased, from $b = 5$, the solution becomes unstable (period two) and then returns to the steady-state at $b \approx 3$, however, as the parameter b is decreased further, the steady-state now follows the lower branch of the hysteresis cycle, corresponding to the other

stable fixed point of the system. Hence it has been shown that the bifurcation diagrams are sensitive to both step size and the choice of initial conditions. It is also evident that it is possible for the steady-state to remain on a path even though that path is unstable, as Figures 3(a) and 3(b) demonstrate.

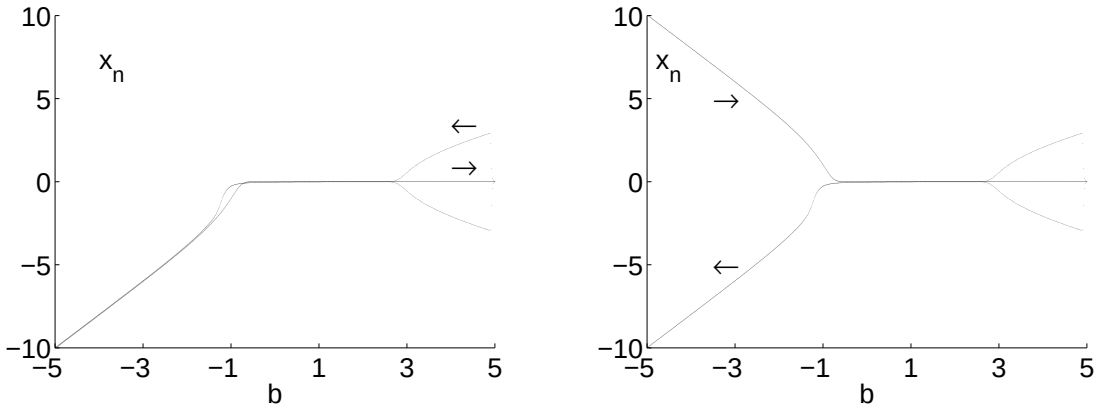

Figure 3: Bifurcation diagrams for system (1) when $\gamma = 0.5$ using a stepsize of 0.01. Parameters b and w are varied simultaneously, b is ramped up then down and parameter w is ramped down then up, $(-5 \leq b \leq 5, -10 \leq w \leq 10)$. (a) The initial condition chosen at $b = -5, w = 10$ is $x(0) = -10$. (b) The initial condition for the same set of parameter values is $x(0) = 10$.

The next section is concerned with a simple chaotic two-neuron module that can display hysteresis and periodic and quasiperiodic behaviour.

3. Stability analysis of a simple two-neuron module

Consider the simple two-neuron module as depicted in Figure 4. The discrete dynamical system used to model the neuromodule is given by

$$x_{n+1} = b_1 + w_{11}\sigma_1(x_n) + w_{12}\sigma_2(y_n), \quad y_{n+1} = b_2 + w_{21}\sigma_1(x_n) + w_{22}\sigma_2(y_n), \tag{2}$$

where x_n, y_n are the activation levels of the neurons; b_1, b_2 are biases; w_{ij} are synaptic weights and $\sigma_1(x)$, $\sigma_2(y)$ are transfer functions. This simple system displays chaos, periodicity and quasiperiodicity, characteristics that are evident in much more complicated neuromodules. Without loss of generality, assume in the work to follow that the weight w_{22} is zero and the transfer functions are defined by the bipolar functions $\sigma_1(x) = \tanh(\alpha x)$, $\sigma_2(y) = \tanh(\beta y)$, this will make the analysis more manageable.

Fixed points of period one, which will correspond to steady-state behaviour, are found by solving the equations, $x_{n+1} = x_n = x$, say, and $y_{n+1} = y_n = y$, say. Hence from system (2),

$$b_1 = x - w_{11}\tanh(\alpha x) - w_{12}\tanh(\beta y), \tag{3}$$

and

$$y = b_2 + w_{21}\tanh(\alpha x). \tag{4}$$

The stability of these fixed points is determined by a linearization technique [13–15]. Each fixed point can be transformed to the origin and the nonlinear terms can be discarded after taking a

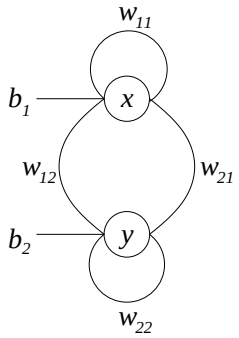

Figure 4: A recurrent two-neuron module.

Taylor series expansion. The Jacobian matrix is given by

$$J = \begin{pmatrix} \frac{\partial P}{\partial x} & \frac{\partial P}{\partial y} \\ \frac{\partial Q}{\partial x} & \frac{\partial Q}{\partial y} \end{pmatrix},$$

where $P(x_n, y_n) = x_{n+1}$, $Q(x_n, y_n) = y_{n+1}$. Therefore

$$J = \begin{pmatrix} \alpha w_{11}\text{sech}^2(\alpha x) & \beta w_{12}\text{sech}^2(\beta y) \\ \alpha w_{12}\text{sech}^2(\alpha x) & 0 \end{pmatrix}.$$

The stability conditions for the fixed points are determined by considering the eigenvalues, trace and determinant of the Jacobian matrix. The characteristic equation is given by

$$\lambda^2 - \alpha w_{11}\text{sech}^2(\alpha x)\lambda - \alpha\beta w_{12}w_{21}\text{sech}^2(\alpha x)\text{sech}^2(\beta y) = 0. \tag{5}$$

The fixed points undergo a fold bifurcation when $\lambda = +1$. In this case, equation (5) gives

$$w_{12} = \frac{1 - \alpha w_{11}\text{sech}^2(\alpha x)}{\alpha\beta w_{21}\text{sech}^2(\alpha x)\text{sech}^2(\beta y)}. \tag{6}$$

The fixed points undergo a flip bifurcation when $\lambda = -1$. In this case, equation (5) gives

$$w_{12} = \frac{1 + \alpha w_{11}\text{sech}^2(\alpha x)}{\alpha\beta w_{21}\text{sech}^2(\alpha x)\text{sech}^2(\beta y)}. \tag{7}$$

The fixed points undergo a Neimark-Sacker bifurcation when $\det(J) = 1$ and $|tr(j)| < 2$. Thus

$$w_{12} = -\frac{1}{\alpha\beta w_{21}\text{sech}^2(\alpha x)\text{sech}^2(\beta y)}. \tag{8}$$

Figure 5 shows a typical stability diagram for system (2) using equations (3) and (4) and equations (6)—(8), and is generated using the Manipulate command in Mathematica [14]. As the slider buttons are moved left and right, the stability diagram alters appropriately in an animated sequence.

There are three main cases to consider for system (2):

CASE 1: Suppose that the parameter $w_{11} = 0$, so neuron x has no self-connection.

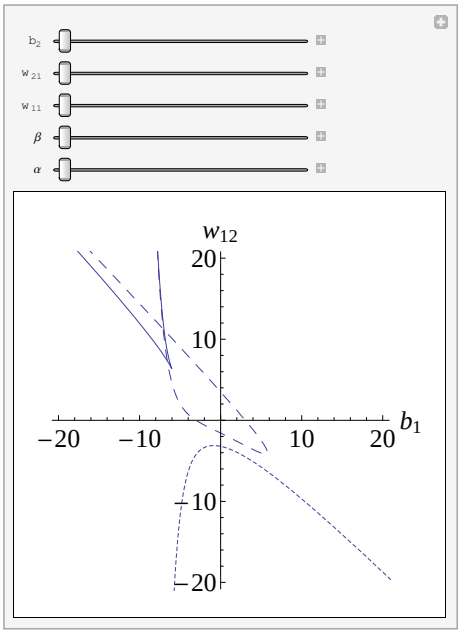

Figure 5: Mathematica parameter slider generated with the Manipulate command. The user can change parameters, α, β, b_2, w_{11} and w_{21} interactively. The solid curve represents the boundary for bistable operation and will be labelled as B^{+1} from now on; the dashed curve is the border for period-doubling bifurcations and will be labelled B^{-1} from now on, and the dotted curve represents the boundary for Neimark-Sacker bifurcations, and will be labelled B^{NS}, from now on.

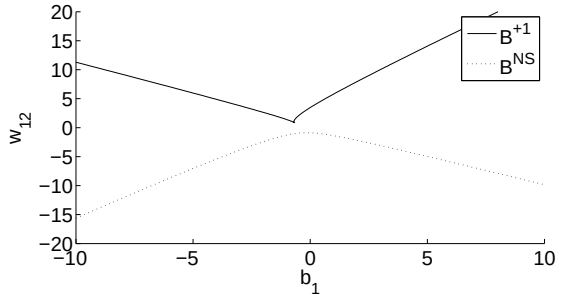

Figure 6: A typical stability diagram when $w_{11} = 0$. In this case, $b_2 = 3$, $w_{21} = 5$, $\alpha = 1$ and $\beta = 0.3$.

A typical stability diagram is plotted in Figure 6. It can be seen that the bistable curve B^{+1} is isolated from the Neimark-Sacker stability curve B^{NS}, say. Two possible bifurcation diagrams are plotted in Figure 7. In Figure 7(a), the parameter b_1 is ramped up from $b_1 = -5$ up to $b_1 = 5$ and then ramped down again for $w_{12} = 5$ and the parameter values listed in the figure. It can be seen that a large counterclockwise hysteresis loop is present for $-4 < b_1 < 1$, approximately, which is in agreement with the bounding bistability curves plotted in Figure 6. In Figure 7(b), the parameter b_1 is ramped up from $b_1 = -5$ up to $b_1 = 5$ and then ramped down again for $w_{12} = -4$ and the parameter values listed in the figure. It can be seen that a large period-2 loop is present for $-3 < b_1 < 4$, approximately, which again agrees with the bounding Neimark-Sacker curve plotted in Figure 6.

CASE 2: Neuron x is a self-excitatory neuron, where $w_{11} > 0$.

A typical stability diagram is plotted in Figure 8. The unstable curve bounded by B^{-1} does

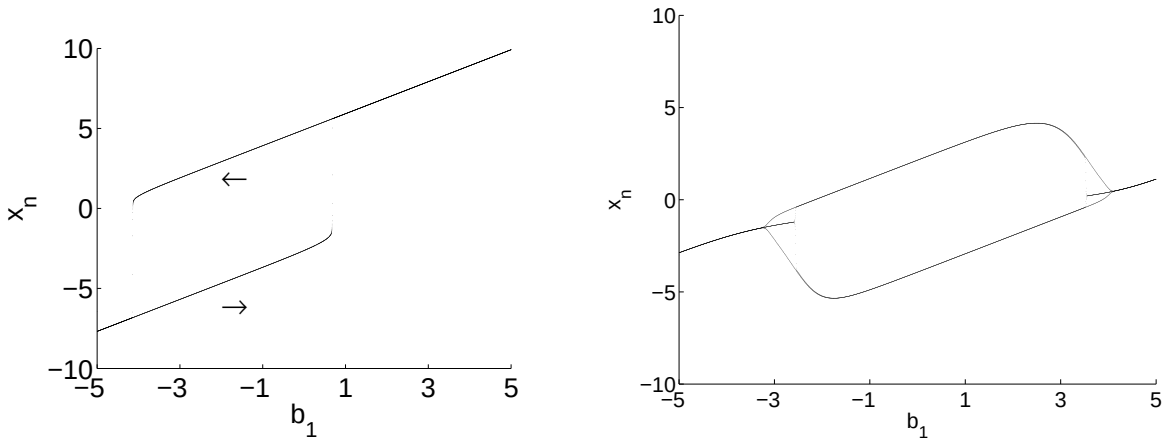

Figure 7: Typical bifurcation diagrams for system (2) when $w_{11} = 0$, $b_2 = 3$, $w_{21} = 5$, $\alpha = 1$ and $\beta = 0.3$ using a stepsize of 0.01. The parameter b_1 is ramped up then down, $-5 \leq b_1 \leq 5$. (a) The parameter $w_{12} = 5$ and the initial conditions are $x(0) = -7$, $y(0) = -2$. (b) The parameter $w_{12} = -4$ and the initial conditions are $x(0) = -3$, $y(0) = -2$.

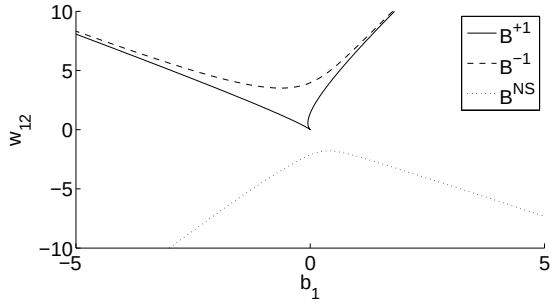

Figure 8: A typical stability diagram when $w_{11} > 0$. In this case, $w_{11} = 1$, $b_2 = 1$, $w_{21} = 2$, $\alpha = 1$ and $\beta = 0.3$.

not affect the bistable operation when $w_{11} > 0$. Two possible bifurcation diagrams are plotted in Figure 9. In Figure 9(a), the parameter b_1 is ramped up from $b_1 = -5$ up to $b_1 = 5$ and then ramped down again for $w_{12} = 5$ and the parameter values listed in the figure. It can be seen that a large counterclockwise hysteresis loop is present for $-3 < b_1 < 1$, approximately, which is in agreement with the bounding bistability curves plotted in Figure 8. In Figure 9(b), the parameter b_1 is ramped up from $b_1 = -5$ up to $b_1 = 5$ and then ramped down again for $w_{12} = -5$ and the parameter values listed in the figure. It can be seen that a large quasiperiodic and periodic loop is present for $-1 < b_1 < 3$, approximately, which again agrees with the bounding Neimark-Sacker curve plotted in Figure 8.

CASE 3: Neuron x is a self-inhibatory neuron, where $w_{11} < 0$.

A typical stability diagram is plotted in Figure 10. The unstable curve bounded by B^{-1} does affect the bistable operation when $w_{11} < 0$. Two possible bifurcation diagrams are plotted in Figure 11. In Figure 11(a), the parameter b_1 is ramped up from $b_1 = -8$ up to $b_1 = 8$ and then ramped down again for $w_{12} = 5$ and the parameter values listed in the figure. It can be seen that a large unstable period-2 cycle has encroached upon the counterclockwise hysteresis loop for $3 < b_1 < 6$, approximately, which is in agreement with the bounding curves B^{+1} and

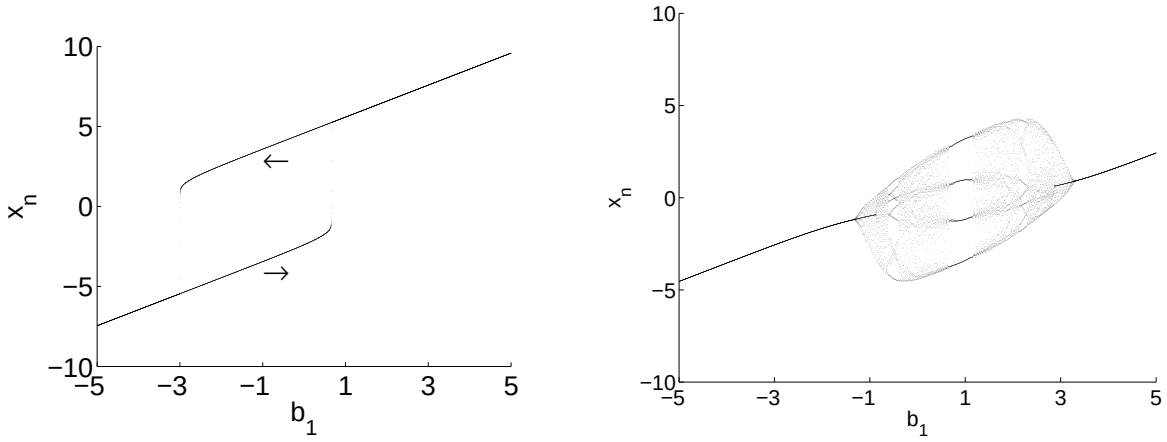

Figure 9: Typical bifurcation diagrams for system (2) when $w_{11} > 0$. In this case, $w_{11} = 1$, $b_2 = 1$, $w_{21} = 2$, $\alpha = 1$ and $\beta = 0.3$. The parameter b_1 is ramped up then down, $-5 \leq b_1 \leq 5$. (a) The parameter $w_{12} = 5$ and the initial conditions are $x(0) = -7$, $y(0) = -1$. (b) The parameter $w_{12} = -5$ and the initial conditions are $x(0) = -5$, $y(0) = -1$.

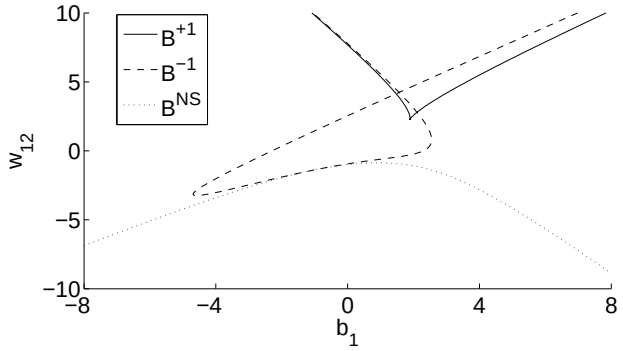

Figure 10: A typical stability diagram when $w_{11} < 0$. In this case, $w_{11} = -2$, $b_2 = -3$, $w_{21} = 5$, $\alpha = 1$ and $\beta = 0.3$.

B^{-1}, plotted in Figure 10. In Figure 11(b), the parameter b_1 is ramped up from $b_1 = -5$ up to $b_1 = 5$ and then ramped down again for $w_{12} = -5$ and the parameter values listed in the figure. It can be seen that a large period-2 loop is present for $-3 < b_1 < 0$, approximately, and a quasiperiodic loop is present for $0 < b_1 < 2$, approximately, which again agrees with the bounding curves B^{-1} and B^{NS}, plotted in Figure 10. One can check that the behavior of a discrete system is quasiperiodic by plotting a power spectrum using a fast Fourier transform.

Now fix the parameter b_1 and vary the parameter w_{12} for the parameter values listed in Figure 10. The parameter b_1 is fixed at $b_1 = 1$ and the parameter w_{12} is ramped down then up for $-10 \leq w_{12} \leq 10$. Figure 12(a) shows the bifurcation diagram obtained when the initial conditions chosen are $x(0) = -7$, $y(0) = -7$ and Figure 12(b) shows the corresponding bifurcation diagram when the initial conditions are $x(0) = 4$ and $y(0) = 2$. In both cases, there is unstable behaviour swamping the bifurcation diagrams.

In the final case, consider system (2) with the parameters listed as in Figure 10 and ramp w_{12} down then up for $5 \leq w_{12} \leq 10$. The initial conditions chosen are $x(0) = 4$ and $y(0) = 2$ in order that a hysteresis cycle will exist, as Figure 13 demonstrates. There is a large open counterclockwise hysteresis cycle. If initial conditions $x(0) = -7$ and $y(0) = -7$ are chosen,

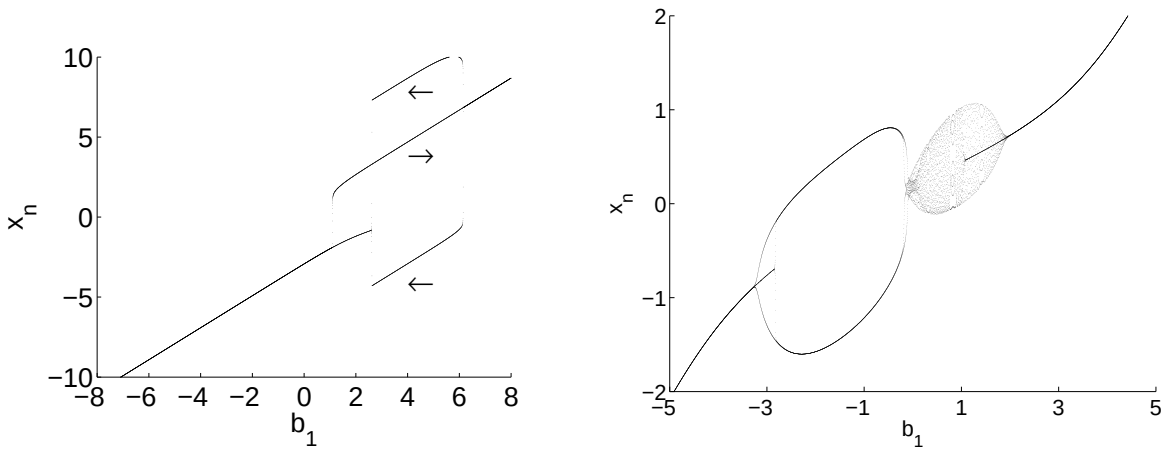

Figure 11: Typical bifurcation diagrams for system (2) when $w_{11} < 0$. In this case, $w_{11} = -2$, $b_2 = -3$, $w_{21} = 5$, $\alpha = 1$ and $\beta = 0.3$. (a) The parameter b_1 is ramped up and down, $-8 \leq b_1 \leq 8$, $w_{12} = 5$ and the initial conditions are $x(0) = -11$, $y(0) = -8$. (b) The parameter b_1 is ramped up and down, $-5 \leq b_1 \leq 5$, $w_{12} = -1$ and the initial conditions are $x(0) = -2$, $y(0) = -8$.

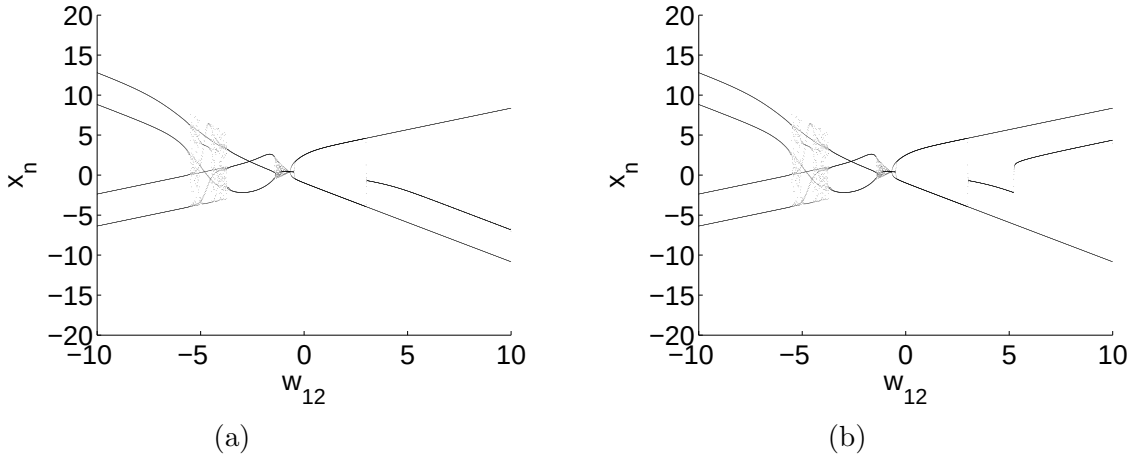

Figure 12: Typical bifurcation diagrams for system (1) when $w_{11} < 0$. In this case, $w_{11} = -2$, $b_2 = -3$, $w_{21} = 5$, $\alpha = 1$ and $\beta = 0.3$. The parameter w_{12} is ramped down and up, $-10 \leq w_{12} \leq 10$, $b_1 = 1$. (a) The initial conditions are $x(0) = -7$, $y(0) = -7$. (b) The initial conditions are $x(0) = 4$, $y(0) = 2$.

then no bistable cycle will form. Thus, once more the system is shown to be history dependent.

4. Conclusions and further work

A stability analysis and feedback mechanism has been implemented to model the dynamics of neurons and simple neuromodules. Feedback is important in artificial neural networks, and is undoubtedly involved in the development of human brains. The dynamics of neurons and simple neuromodules demonstrate a broad range of possible behaviours for these systems. It has been shown that the dynamics are dependent not only on the history, but also on the initial conditions chosen at the start of the simulations, the step-size used in the simulations, the number of varying parameters and the extent to which those parameters are varied. This work clearly demonstrates that the stability analysis and the simultaneous plotting of bifurcation

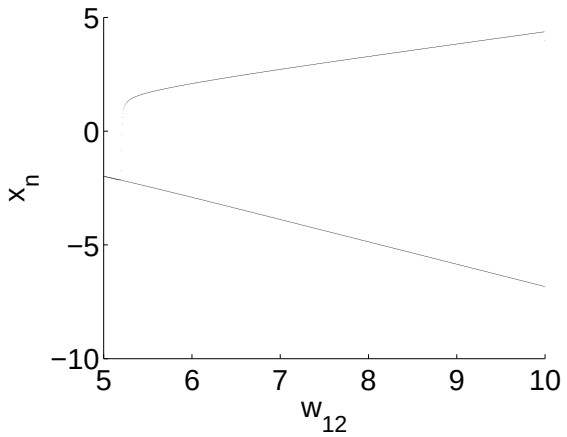

Figure 13: A bifurcation diagram for system (1) for the parameter values $w_{11} = -2$, $b_2 = -3$, $w_{21} = 5$, $\alpha = 1$ and $\beta = 0.3$. In this case, w_{12} is ramped down from $w_{12} = 10$ to $w_{12} = 5$ and then ramped back up again. The initial conditions are $x(0) = 4$, $y(0) = 2$. There is a large open bistable region for $w_{12} > 5$, approximately.

diagrams with feedback are required to fully understand the dynamics involved in these simple systems.

It is well known that stochastic resonance can cause jumps between attractors in the human brain. There appears to be little research on how history can affect jumps between different steady states in the brain. This work indicates the need to investigate feedback and its affect on neuronal models.

Future work will concentrate on feedback in highly nonlinear systems, where there are expected to be bifurcations involving multiple—fixed points, limit cycles and chaotic attractors.

References

[1] Fitzhugh R (1961) Impulses and physiological states in theoretical models of nerve membranes. Biophys 1182 445–466.

[2] Nagumo J, Arimoto S,Yoshizawa S (1970) An active pulse transmission line simulating 1214-nerve axons. Proc IRL 50 2061–2070.

[3] Hodgkin AL, Huxley AF (1952) A qualitative description of membrane current and its application to conduction and excitation in nerve. J Physiol 117 500–544. Reproduced in Bull Math Biol 52 (1990) 25–71.

[4] Borresen J, Lynch S (2009) Neuronal computers. Nonlinear Anal Theory Meth & Appl 71 2372–2376.

[5] Ashwin P, Borresen J (2004) Encoding via conjugate symmetries of slow oscillations for globally coupled oscillators. Phys Rev Ev 70 026203.

[6] Ashwin P, Borresen J (2005) Discrete computation using a perturbed heteroclinic network. Phys Letts A 347 208–214.

[7] Ashwin P, Orosz G, Borresen J (2010) Heteroclinic Switching in Coupled Oscillator Networks: Dynamics on Odd Graphs. Nonlinear Dynamics and Chaos: Advances and Perspectives 31–50.

[8] Hopfield JJ (1982) Neural networks and physical systems with emergent collective computational abilities,. Proc National Academy of Sciences 79 2554–2558.

[9] Lynch S, Borresen J (2012) Binary half adder using oscillators. International Publication Number, WO 2012/001372 A1 1-57.

[10] Lynch S, Borresen J (2012) Binary half adder and other logic circuits. UK Patent Number GB 2481717 A 1-57.

[11] Borresen J, Lynch S (2012) Oscillatory threshold logic, submitted to PLoS ONE (preprint) (2012).

[12] Hirsch M (1991) Network dynamics: Principles and problems in: Neurodynamics, eds. F. Paseman and H.D. Doebner World Scientific 183–185.

[13] Lynch S (2004) Dynamical Systems with Applications using MATLAB Springer.

[14] Lynch S (2007) Dynamical Systems with Applications using Mathematica Springer.

[15] Lynch S (2010) Dynamical Systems with Applications using Maple, 2nd ed Springer.

[16] Benzi R, Sutera A, Vulpiani A (1981) The mechanism of stochastic resonance. J Phys A Math Gen 14L 453.

[17] Fauve S, Reslot F (1983) Stochastic resonance in a bistable system. Phys Lett 97A 5–7.

[18] Tucknell HC (1989) Stochastic Processes in the Neurosciences SIAM.

[19] Zaikin A, Garcia-Ojalvo J, Bascones R, Ullner E, Kurths J (2003) Doubly stochastic coherence via noise-induced symmetry in bistable neural models. Phys Rev Lett 90 030601.

[20] Drover JD, Ermentrout B (2003) Nonlinear coupling near a degenerate Hopf (Bautin) bifurcation. SIAM J Appl Maths 63 1627–1647.

[21] Lynch S, Christopher CJ (1999) Limit cycles in highly nonlinear differential equations. J of Sound and Vibration 224 505–517.

[22] Duke W, Pritchard WS (ed) (1991) Proc Conf on Measuring Chaos in the Human Brain World Scientific.

[23] Dafilis MP, Liley DTJ, Cadusch PJ (2001) Robust chaos in a model of the electroencephalogram: Implications for brain dynamics. Chaos 11 474–478.

[24] Pantev C, Elbert T, Lutkenhöhner B (ed.) (1995) Oscillatory Event-Related Brain Dynamics Plenum.

[25] Pasemann F, Neuromodules: A dynamical systems approach to brain modelling, Supercomputing in Brain Research: From tomography to neural networks. ed. Hermann H. et al. World Scientific 331.

[26] Pasemann F (1997) A simple chaotic neuron. Physica D 104 205–211.

[27] Pasemann F (1999) Driving neuromodules into synchronous chaos. Lecture notes in computer science 1606 377–384.

[28] Pasemann F (2002) Complex dynamics and the structure of small neural networks. Network: Comput Neural Syst 13 195–216.

[29] Pasemann F, Hild M, Zahedi K (2003) SO(2)-networks as neural oscillators. Computational methods in neural modeling 2686 144–151.

[30] Yuan Z, Hu D, Huang L (2005) Stability and bifurcation analysis on a discrete-time neural network. J Comp and Appl Maths 177 89–100.

[31] Kuznetzov YA (2004) Elements of Applied Bifurcation Theory 3rd ed Springer.

[32] Guo S, Tang X, Huang L (2008) Stability and bifurcation in a discrete system of two neurons with delays. Nonlin Anal: Real World Appl 9 1323–1335.

[33] Redmond BF, Le Blanc VG, Longtin A (2002) Bifurcation analysis of a class of first-order nonlinear delay-differential equations with reflectional symmetry. Physica D 166 131–146.

[34] Xu X 92008) Local and global Hopf bifurcation in a two-neuron network with multiple delays. Int J of Bifurcation and Chaos 18 1015–1028.

[35] Gaver DP, Jacobs PA, Carpenter RL, Burkhart JG (1997) A mathematical model for intracellular effects of toxins on DNA adduction and repair. Bull Math Biol 59 89–106.

[36] Lynch S (2005) Analysis of a blood cell population model. Int J of Bifurcation and Chaos 157 2311-2316.

[37] Meyer-Lindenberg A, Ziemann U, Hajak G, Cohen L, Berman KF (2002) Transitions between dynamical states of differing stability in the human brain. Proc Natl Acad Sci USA 99 10948–10953.

[38] Göcke M (2002) Various concepts of hysteresis applied in economics. J Econ Surveys 16 167–188.

[39] Go TH, Lie FAP (2008) Analysis of wing rock due to rolling-moment hysteresis. J of Guidance Control and Dynamics 31 849–857.

[40] Borresen J, Lynch S (2002) Further investigation of hysteresis in Chua's circuit. Int J of Bifurcation and Chaos 12 129–134.

[41] Scott SK (1994) Oscillations, Waves and Chaos in Chemical Kinetics Oxford.

[42] Nejad LAM, Wagenblast R (1999) Time dependent chemical models of dark spherical clouds, Astronomy and Astrophysics 350 204–229.

[43] Fisher GH (1967) Measuring ambiguity. Amer J Psych 80 541–547.

[44] Arrow H (1997) Stability, bistability, and instability in small group influence patterns. J of Personality and Soc Psych 72 75–85.

[45] Izhikevich EM (1998) Multiple cusp bifurcations. Neural Networks 11 495–508.

[46] Steele AL, Lynch S, Hoad JE (1997) Analysis of optical instabilities and bistability in a nonlinear optical fibre loop mirror with feedback. Optics Comm 137 136–142.

[47] Lynch S, Steele AL (2011) Nonlinear optical fibre resonators with applications in electrical engineering and computing. Applications of Nonlinear Dynamics and Chaos in Engineering, Santo Banerjee, Mala Mitra, Lamberto Rondoni (Eds.) Springer 1 65–84.